Beam-Based Alignment and Tuning Procedures for e^+e^- Collider Final Focus Systems*

F. BULOS, D. BURKE, R. HELM, J. IRWIN, A. ODIAN, G. ROY, R. RUTH, N. YAMAMOTO
Stanford Linear Accelerator Center Stanford University, Stanford, California 94309

Abstract

For future linear colliders, with very small emittances and beam sizes and demanding tolerances on final focus system alignment and magnet errors, it becomes increasingly important to use the beam as a diagnostic tool. We report here procedures we have identified and will be implemented in the Final Focus Test Beam at SLAC incorporating i) quadrupole strength changes, ii) central orbit modifications, iii) spot size measurements, and iv) beam stability monitoring.

I. ANALYSIS OF BEAM CENTROID

A. Quadrupole Alignment

Each quadrupole will be mounted on a magnet mover with vertical and horizontal range of $\pm 3mm$ and setting accuracy of $\leq 1\mu$. Alignment will be monitored by a wire alignment system, in which sensors indexed to each quadrupole will detect position relative to a system of stretched wires. The absolute positioning of the wires is expected to be $\sim \pm 100\mu$ and the location of quadrupole magnetic centers relative to the wires is expected to be $\sim \pm 10\mu$. Relative motions in the $1\,\mu$ range should be detectable. [1] If a quadrupole of inverse focal length k_i is varied by an amount $\pm\Delta k_i$, the trajectory difference at a downstream position monitor is

$$\Delta x_j = 2R_{12}^{ji}\Delta k_i x_{ci} \qquad (1)$$

where x_{ci} is the offset of the quadrupole relative to the beam and R_{12}^{ji} is the x, x' matrix element from i to j, assumed known from the optics model. The value of x_{ci} may be found by a least-squares fit to measurements of Δx_j at several monitors.

Figure 1 shows the layout of the FFTB. Beamline segments may be rotated about hinge points (HP), located at the beginning of the system or at vertices of the bends; base quadrupoles (BQ) are quadrupoles near the hinge points which will be kept fixed relative to the wire alignment system; an alignment segment is the straight line defined by a hinge point and the next base quadrupole.

Figure 2 depicts the alignment procedure. The quadrupoles in a given segment are varied one at a time and each with the exception of the base quadrupole is moved onto the beam line according to Eq. (1). Then the segment is "hinged" into alignment with the base quadrupole by steering at the hinge point and moving each quadrupole except the base quadrupole in proportion to its distance from the hinge point. The procedure is then repeated for each successive segment.

If we assume that position measurement errors are random and uncorrelated, with an rms value of $\sigma_{\rm bpm}$, then the uncertainty σ_{ci} in the determination of x_{ci} is

$$\sigma_{ci} = S_i\sigma_{\rm bpm} = \left(2\Delta k_i (\sum_{j>i} R_{12}^{ji\,2})^{1/2}\right)^{-1}\sigma_{\rm bpm} \qquad (2)$$

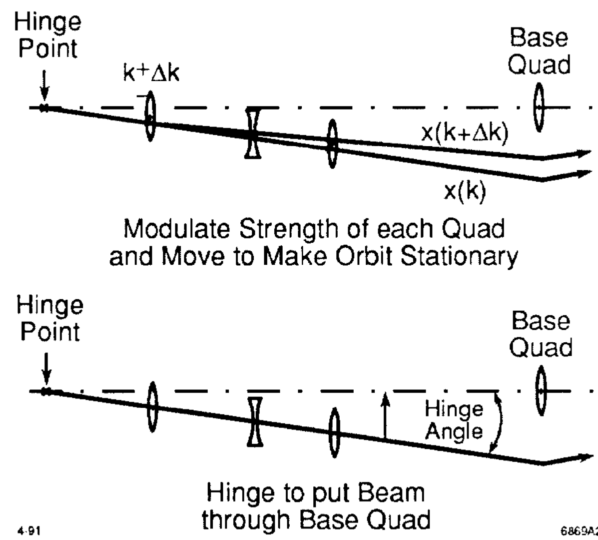

Figure 2. Quadrupole Alignment Procedure

Values of S_i for some of the most sensitive FFTB quadrupoles are compared to alignment tolerances in Table 1. The tolerance is the alignment error which would make either a 2% increase in spot size at the IP, or a 1σ maximum orbit perturbation anywhere in the lattice, whichever is smaller. We conclude that if the position monitor precision is $\sim 1\mu$ then all the quadrupoles can be aligned nearly to tolerance. The globalcorrection methods described below should then be able to compensate for residual errors.

B. Quadrupole Tuning

Quadrupole strengths can be probed by orbit bumps. The FFTB has six horizontal and six vertical dipoles for

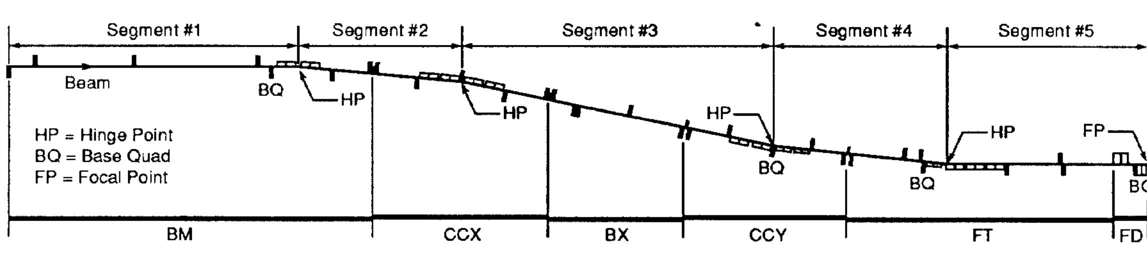

Figure 1. FFTB Alignment Segments

* Work supported by Department of Energy contract DE–AC03–76SF00515.

Table 1. Beam-based Quadrupole Alignment
Tolerances and sensitivites are given in microns.

Segment	Section	Element	Horizontal		Vertical	
			Toler.	Sensi.	Toler.	Sensi.
1	BM	Q5	110	.74	4.5	.04
		QA1	60	.42	20	.30
2	CCX	QN2	2.9	1.7	2.0	.36
		QN1	.71	.57	4.0	.63
3	BX	QT2	10	2.5	4.4	.53
		QT3	1.3	.55	30	1.9
	CCY	QM1	.65	.75	1.2	2.1
		QM2	1.1	1.3	.31	.81
4		QM1	.65	.73	1.1	2.6
	FT	QM1	1.3	.53	2.0	2.1
		QC5	4.4	.9	1.2	1.0
5	FD	QC2	15	1.5	4.8	6.8
		QC1	44	3.6	5.5	4.9

launching and terminating orbit bumps. The fact that each major subsection (CCX, BX, CCY, and FT of Fig. 1) has π phase advance enhances the sensitivity of this process. The transfer matrix between points separated by π is

$$\begin{pmatrix} -m, & 0 \\ r, & -\frac{1}{m} \end{pmatrix}$$

The linear combination of $x_1 + \frac{1}{m}x_2$ should be independent of both the initial position and slope of the beam at x_1. This condition can be checked alternately for x'-, x-, y'- and y-bumps, yielding four conditions on intermediate quadrupole strengths. Since all of these π sections have less than four contributing quadrupoles (end quadrupoles affect only the R_{21} element), the strengths of the intermediate quadrupoles can be checked. The amplitude of the bumps is chosen as large as possible subject to the constraint that the beam clear the beam-pipe by 8σ. We can check the setting error of the end quadrupoles by studying a π section between beta minimum points (see Fig. 3) for which the former end quadrupoles are now intermediate. One quadrupole located between the first dipole and the first CCX sextupole must be verified by launching a bump of known strength and requiring the appropriate displacement at the sextupole. All other quadrupoles with the exception of the final quadrupoles can be checked with the method we have described.

C. Sextupole Alignment

For a sextupole pair define $\Delta x_S = 0.5(\Delta x_1 + \Delta x_2)$ and $\Delta x_A = \Delta x_1 - \Delta x_2$. A non-zero Δx_A is equivalent to a quadrupole setting error at the sextupole position and can be detected with the same methods described above. Non-zero Δy_A creates a skew quadrupole error which can be detected if, for example, vertical motion appears in the presence of a horizontal bump.

Table 3 summarizes the sensitivity of the method in the FFTB lattice.

D. Stability Monitoring

During and following the setting of global correctors described in Sec. 4, it is important that the system remain stable. We discuss here methods to stabilize the most sensitive aberrations.

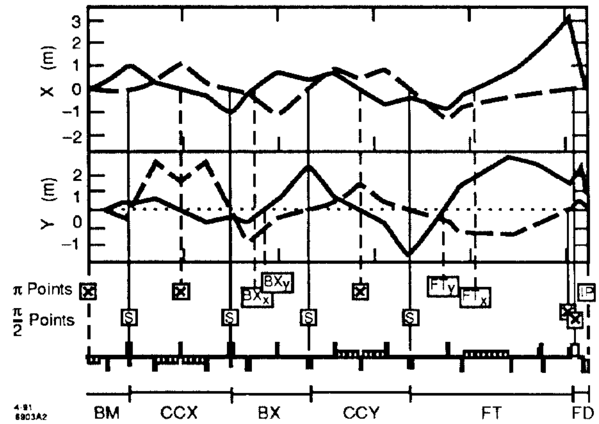

Figure 3. FFTB Orbit Bumps for Quadrupole Tuning

Table 2. Beam-based Quadrupole Tuning

Quad	Bump	$\frac{\Delta k}{k}$ Sensitivity	$\frac{\Delta k}{k}$ Tolerance
QN2	2 mm/X at SF1	6.2×10^{-4}	1.2×10^{-3}
QN1	100 μrad/X' at SF1	6.2×10^{-5}	2.1×10^{-2}
QT2	200 μrad/Y' at SF1	9.8×10^{-5}	1.5×10^{-3}
QT3	200 μrad/X' at SF1	5.6×10^{-5}	5.1×10^{-4}
QM1	0.7 mm/X at SD1	2.9×10^{-4}	6.7×10^{-4}
QM2	500 μrad/X' at SD1	2.7×10^{-4}	2.7×10^{-2}
QN3	2 mm/ X at SF1	2.5×10^{-4}	3.3×10^{-4}
QT1	2 mm/ X at SF1	1.4×10^{-4}	1.9×10^{-4}
QT4	3 mm/Y at SD1	1.7×10^{-4}	2.6×10^{-4}
QM3	3 mm/Y at SD1	5.8×10^{-5}	8.8×10^{-5}

Table 3. Beam-based Sextupole Alignment

				Vertical		
SEXT	Bump Spec	Sens.	Toler.	Bump Spec	Sens.	Toler.
SF1	2 mm/X	1.4 μ	3.5 μ	2 mm/X	2.9 μ	3.5 μ
SD1	3 mm/Y	0.9 μ	0.9 μ	3 mm/Y	0.8 μ	1.4 μ

Dispersion arises whenever the beam is off axis in an element which is a source of chromaticity. By monitoring the beam at large chromatic sources, the final doublet and the sextupoles, and maintaining a constant beam position at these points, the dispersion can be stabilized for as long as one can rely on the stability of the BPM readings. For the duration of the stability time, the BPMs at the final doublet will be required to resolve a change of $2\,\mu$ for the FFTB, $.2\,\mu$ for the next linear collider (NLC).

Normal and skew quadrupole aberrations arise when the beam position changes at the sextupoles. In this case it is the sum of the BPM readings at each sextupole pair which must be held constant. The sum reading of the two BPMs is quite insensitive to charge distribution because the sextupoles are at $-I$ with respect to one another and hence the beam distribution at the second sextupole is the mirror image of the distribution at the first. The precision of the BPMs must be $1\,\mu$ for the FFTB, $.1\,\mu$ for NLC. [2]

II. ANALYSIS OF INTERMEDIATE SPOT SIZES

A. *Matching Incoming Beam Optical Functions*

Initially, the incoming β, α, and beam emittance are measured using a special configuration of quadrupole strengths in the beta match section (BM). The proper strengths for the match are then reckoned and set. This setting can be verified after the beam-based quadrupole alignment and tuning have been performed by observing the beam size at the beta minima in the BX section (π points of Fig. 3). By symmetrically varying the strength of the first and last quadrupole in the CCX section, so as not to change the dispersion function in BX, the beam size at BXx should vary according to

$$\frac{\sigma^2}{\sigma_0^2} = 1 + (\beta_Q \Delta k - \alpha_Q)^2$$

The beta match section can be adjusted until $\alpha_Q = 0$ and β_Q has the desired value.

B. *Removing Incoming Dispersion*

By measuring σ_0 above as either a dispersion knob or Δx_S or Δy_S defined in section 2.3 is varied, the system can be tuned so that the horizontal dispersion is zero at BXx and the vertical dispersion is zero at BXy. This is appropriate since these points are image points of the IP for their respective plane.

C. *Removing Incoming Coupling*

The beam delivered to a final focus system may contain coupling between the horizontal and vertical plane. Coupling at the end of the SLAC linac is thought to be about 10%. In general such a coupling may be specified with four parameters. We introduce parameters s_1 to s_4 defined by a transfer matirx or through coupling terms in the beamline Hamiltonian at the focal point,

$$V = s_1\sqrt{\beta_x^*\beta_y^*}x'y' + s_2\sqrt{\frac{\beta_x^*}{\beta_y^*}}x'y + s_3\sqrt{\frac{\beta_y^*}{\beta_x^*}}xy' + s_4\sqrt{\frac{1}{\beta_x^*\beta_y^*}}xy.$$

Note that the parameters s_i are all dimensionless. Only s_1, s_2, and s_3 affect the beam size at the IP. s_2 affects only the horizontal beam size. Since the emittance ratio, $\frac{\epsilon_y}{\epsilon_x}$, is 0.1 in the FFTB and 0.01 in the NLC, the effect of s_2 will be negligible. The term s_3 represents a rotation of the beam profile, the term s_1 represents vertical beam size blow up at the FP as shown in Fig. 4a.

At the point BXy or FTy where $\phi_x - \phi_x^* = \frac{\pi}{2} + n_x\pi$ and $\phi_y - \phi_y^* = n_y\pi$, s_1 and s_3 exchange roles as shown in the Fig. 4b. We can measure the coupling parameters s_1 and s_3 at BXy or FTy and use skew quadrupoles in the beta match section to cancel incoming coupling.

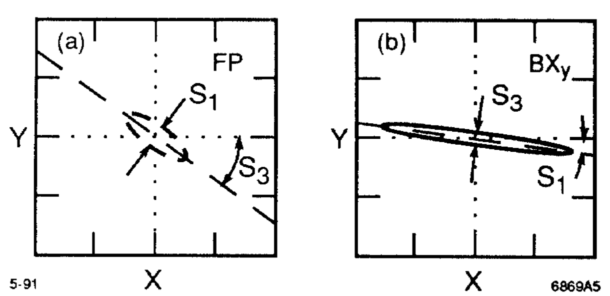

Figure 4. FFTB π Point Beam Profiles

III. ANALYSIS OF FINAL SPOT SIZE

After the foregoing techniques have been used, global correctors will be used to cancel residual aberrations at the interaction point using measurement of the position, size and orientation of the beam at the focal point. We itemize the low order aberrations still requiring correction according to four distinct time scales.

Position jitter in the quadrupole elements of the line will displace the final spot. Correction is carried out by a horizontal and vertical steering dipole placed at the final quadrupole. The time scale τ_0 is determined by feedback requirements and is estimated to be about 15 pulses.

Two steering correctors which control beam position in the final doublet are used to correct dispersion. The time τ_1 is determined by the stability time of BPMs used to maintain postion stability at the final doublet and the sextupoles.

Trim quadrupoles and a skew quadrupole at the final doublet are used to correct waist position (normal quadrupole error) in both planes and coupling (skew quadrupole error). Correction orbit bumps can be used to confirm alignment of the CCS, and with them it may be possible to extend the time scale τ_2 for normal and skew quadrupole effects beyond the BPM stability time τ_1.

The fourth time scale, τ_3, includes chromaticity correction, and two sextupoles and two skew sextupoles in the final transformer to correct sextupolar terms coming from quadrupole imperfections. These corrections are expected to be small and have a yet longer time scale ($\tau_3 \gg \tau_2$) determined by the stability of magnet power supplies.

There are a set of correctors which are used for the matching of the incoming beam from the linac into the final focus system. Four of them will perform the matching of the beta and alpha functions, two will control the dispersion function, and two will control the principal coupling terms. The time scale will depend on the stability of the linac.

IV. CONCLUSION

NLC designs exist which eliminate high order aberrations. The linear modules in these designs need to be optimized to improve tolerances associated with the appearance of low order aberrations. These tolerances are very small by present standards, and beam-based alignment and tuning techniques will be crucial in achieving them. We have described techniques which will be used for the Final Focus Text Beam now under construction at SLAC. [3] If BPMs and BSMs (beam size monitors) can be designed to operate to the required precision, we believe the procedures we have outlined can be used to successfully align and tune these systems.

REFERENCES

[1] R. Ruland and G. Fischer, The Proposed Alignment System for the Final Focus Test Beam at SLAC, SLAC-PUB-5236 (1990)

[2] G. Roy and J. Irwin, Tolerances of Two Next Generation e^+e^- Linear Collider Final Focus System Designs, Snowmass Proceedings (1990)

[3] D. Burke, The Final Focus Test Beam Project at SLAC, NGR5, These Proceedings